

^(b)Present address: Indiana University Cyclotron Facility, Bloomington, Ind. 47401.

¹A substantial fraction of the charged-pion photoproduction on the nucleon is nonresonant. However, many of the pions produced in *nuclei* by photons will subsequently interact through Δ formation.

²R. D. McKeown, S. J. Sanders, J. P. Schiffer, H. E. Jackson, M. Paul, J. R. Specht, E. J. Stephenson, R. E. Segel, and R. P. Redwine, *Phys. Rev. Lett.* **44**, 1033 (1980), and to be published. Note that the conclusion of

that work bears on pion absorption (a Δ -decay mode), whereas we are addressing the common elements of γ and π reactions in this Letter.

³J. Arends, J. Eyink, H. Hartmann, A. Hegerath, B. Mecking, G. Nöldeke, and H. Rost, to be published.

⁴D. Ashery, *Nucl. Phys.* **A335**, 385 (1980).

⁵J. Arends, J. Eyink, H. Hartmann, A. Hegerath, B. Mecking, G. Nöldeke, and H. Rost, in *Photopion Nuclear Physics*, edited by P. Stoler (Plenum, New York, 1979), p. 275.

Excitation of Helium Atoms by Positron Impact

P. G. Coleman and J. T. Hutton

Center for Positron Studies, The University of Texas at Arlington, Arlington, Texas 76019

(Received 7 July 1980)

Excitation cross sections for positrons of energies up to 10 eV above threshold scattered in the forward direction by helium atoms have been measured directly by use of time-of-flight spectrometry. The results indicate that the scattering is dominated by excitation of the 2^1S state and that there exists a strong small-angle lobe in the angular distribution of the scattered positrons.

PACS numbers: 34.80.Dp, 34.90.+q

The partition of the total scattering cross section for positron collisions with atoms and molecules is of fundamental importance. In addition to the unique positronium-formation process, the cross sections for positron-atom excitation and ionization are of interest because of the difference between them and the equivalent electron cross sections. For example, the excitation of triplet levels through exchange will be absent in the case of positrons. The energy-dependent inelastic cross sections govern the slowing-down process for positrons in gases and knowledge of them is prerequisite to the full interpretation of the features of measured positron-lifetime spectra in gases, such as the positronium-formation fraction. The same knowledge is essential when considering the fate of galactic positrons which may form positronium or excite or ionize gas molecules prior to annihilation and the emission of the characteristic radiation which has been detected on Earth.¹

Recently Griffith *et al.*² determined that at intermediate energies (up to 500 eV) the dominant positron-helium inelastic collision process is ionization, but no direct measurement of a positron inelastic cross section has been reported to date.

In this Letter measurements of cross sections are presented for the excitation of helium by pos-

itrons of energies up to 10 eV above threshold (20.6 eV) accompanied by deflection of the positrons through forward angles of up to 70° . In these energy and angular ranges positrons scattered following excitation collisions are readily distinguished from those scattered through elastic, ionization, and positronium-formation channels.

The time-of-flight (TOF) apparatus used for the present measurements has been described elsewhere.³ Slow positrons, accelerated to the desired mean energy and having an energy spread of about 1 eV, are timed sequentially along a 25.3-cm-long flight path from source to Channeltron detector under the influence of a strong, uniform, axial magnetic field (150 G) in a chamber evacuated in 10^{-7} Torr by two 6-in.-diam diffusion pumps. The initial direction of the accelerated positrons is essentially axial^{3,4}; for the current measurements most of the positron's energy is derived from the axial electrostatic field. The timed beam is 3 mm in diameter and of intensity 0.4/sec, found by use of an MgO-coated grid moderator. The intensity was increased to 1.2/sec by replacing the MgO with a 50%-transmission annealed tungsten mesh.⁵

The accumulation of a time spectrum for positrons *in vacuo*, with use of a standard fast-timing electronics (time-to-amplitude converter-

multichannel analyzer) system,³ was followed by the collection of a second spectrum with helium gas at a pressure of 0.2 Torr in a 10-mm-long gas cell situated at the beginning of the flight path. A pressure differential of at least $10^4:1$ was maintained and over 99% of the scattering occurred within the cell. A typical TOF spectrum collected with helium in the cell is shown in Fig. 1. The peak on the right-hand side of the spectrum contains those positrons not scattered in the cell. The secondary peak is due to positrons which have lost a discrete amount of energy through excitation of helium atoms and have proceeded in the forward direction to the detector.

The intensities I_{ex} of the secondary peaks were straightforwardly measured from the TOF spectra, which were first subjected to signal-restoration and background-subtraction procedures.^{6,7} Three examples of peaks for incident positron energies 24, 25, and 28 eV are presented in Fig. 2. The signal level on both sides of the secondary peaks in these and other like spectra is essentially zero and it is reasonable to assume that the number of elastically scattered positrons under the peaks is negligible and that the secondary peaks contain only positrons which have excited helium atoms, predominantly to the 2^1S state. In Fig. 2 the TOF's corresponding to energy losses of 20.6 eV and zero angular deflection are indicated and in all cases the positrons of the secondary peaks are consistent with this energy loss. Note that 2^3S excitation, with a threshold at 19.8 eV,

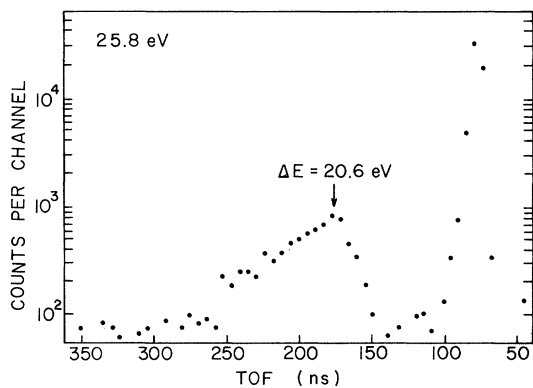


FIG. 1. TOF spectrum showing primary (unscattered) and secondary (excitation) peaks, for positrons of mean incident energy 25.8 eV. Background component subtracted, channels combined in groups of four. Note the logarithmic scale. Helium cell pressure is 0.25 Torr; run time is 10^5 sec. Note that the TOF for $\Delta E = 24.6$ eV is 381 nsec (off scale).

is not important here because of the absence of exchange. Although there may be contributions to the secondary peaks from n^1P channels, these do not appear as peaks at the appropriate TOF's, and most probably they are too small to be distinguished above the statistical fluctuations of the current data. Also indicated in Fig. 2 are the calculated TOF's of positrons which ionize helium atoms. It is clear that below 30 eV, positrons scattered through excitation and ionization channels are readily distinguished.

In all the spectra accumulated, most of the width of the excitation peak is accounted for by adding the natural time width of a spectrum peaked at $E_{inc} - 20.6$ eV to the timing spread introduced because the excitation collisions occur at any point in the gas cell (e.g., $30 + 12$ nsec for the example of Fig. 1). The difference between these contributions and the measured widths is attributed to scattering through angles typically less than 20° . In all cases TOF's corresponding to excitation followed by scattering through forward angles of at least 60° were monitored, but the absence of significant long-time "tails" on the measured excitation peaks indicates that the angular distribution of the scattered positrons is strongly peaked in the forward direction.

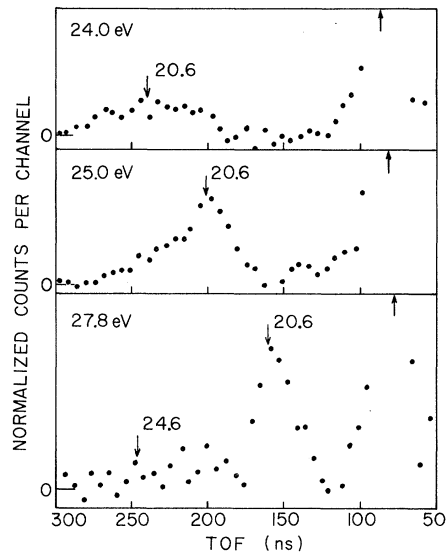


FIG. 2. TOF (gas) spectra showing excitation peaks for incident positron energies of 24.0, 25.0, and 27.8 eV. The positions of the primary peaks are indicated by arrows, as are the TOF's corresponding to $\Delta E = 20.6$ eV and, when on scale, $\Delta E = 24.6$ eV. The data are combined in four-channel groups, have background components subtracted, and are normalized to the same run time and I_i values.

At incident energies above 30 eV, scattered positrons having lost 24.6 eV or more in ionizing helium atoms appear on the time spectra in a peak which overlaps the excitation peak, as illustrated in Fig. 3. The sketched shapes of the excitation peaks in Fig. 3 are based on the assumptions that the cross section is approximately independent of energy between 30 and 50 eV, that the angular distribution of the positrons after excitation does not become less sharply forward peaked with increasing energy, and that the contribution from elastically scattered positrons is again negligible. The intensity of the ionization peak and the extent of the overlap increase as the incident energy increases, and at 50 eV the excitation peak is swamped by the ionization peak. Note that the ionization peak has a relatively long "tail" corresponding to energy losses of more than 24.6 eV and/or larger-angle scattering. Lower bounds on the ionization cross section, deduced from spectra such as those in Fig. 3, range from $0.05\pi a_0^2$ at 30 eV to $0.48\pi a_0^2$ at 50 eV.

The excitation cross sections Q_{ex} shown in Fig. 4 are only for incident positron energies at which the ionization and excitation peaks are straightforwardly separable, and are deduced by use of the thin-target formula

$$Q_{ex} = Q_T I_{ex} / I_s, \quad (1)$$

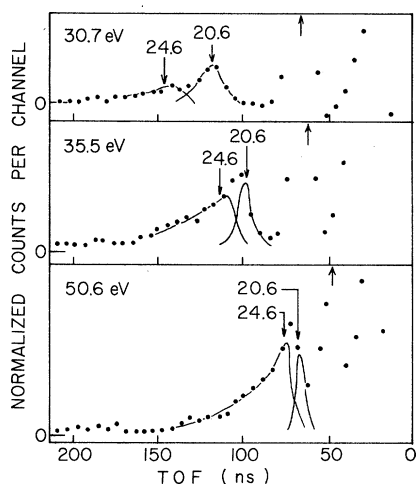


FIG. 3. TOF (gas) spectra illustrating three stages leading to the eventual domination of the excitation peak by the ionization peak, at positron energies of 30.7, 35.5, and 50.6 eV. Presentation of the data follows the format of Fig. 2. The solid lines represent the most likely shapes of the two component peaks which add to give the observed spectra.

where Q_T is the appropriate total cross section,^{4,8,9} I_{ex} is the intensity of the secondary peak in positrons per second, and I_s is the total rate at which positrons are scattered through all channels. I_s is calculated from the formula

$$I_s = I_i [1 - \exp(-nlQ_T)], \quad (2)$$

where I_i is the intensity of the incident beam, measured from the vacuum spectrum, and nl is the helium-atom number density times the cell path length. I_i was measured before and after the accumulation of the gas spectrum and a mean value used. The product nl was determined by measuring the attenuation of beams with mean energies in the range 11–15 eV with use of the same gas pressure, but with the lowest-possible axial-magnetic-field strength; in this energy region, the elastic scattering is predominantly large angle,¹⁰ and use of the difference in vacuum and gas signal rates for I_s in (2) yields the product nl . It was found, however, that between 20 and 30 eV the numbers of elastically scattered positrons whose TOF's remain within the limits of the primary peak were insignificant, indicating predominantly large-angle elastic scattering.

The differential cross section for 2^1S excitation of helium by electron impact is large at small angles in the incident-energy range 22–30 eV,^{11,12} decreasing to almost zero at 60° , but there is also a significant large-angle lobe to the angular distribution similar in size to the small-angle lobe. The cross sections reported herein are for excitation followed by deflection into the forward lobe and represent lower bounds on the total ex-

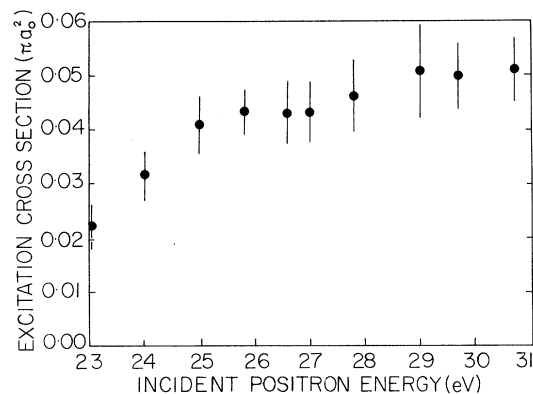


FIG. 4. Cross sections for the excitation of helium by positron impact followed by scattering into the forward direction (see text). Error bars represent statistical and systematic uncertainties. The results were obtained using both MgO and tungsten moderators.

citation cross section.

If one partitions the detailed total cross sections of Stein *et al.*⁹ in the manner of Coleman *et al.*,¹³ then the total-excitation-cross-section values at 23 and 24.6 eV are about $0.03\pi a_0^2$ and $0.05\pi a_0^2$, respectively, which are close to the values shown in Fig. 4 and which suggest that the angular distribution for positrons at these energies may be more forward peaked than for electrons. From an analysis of positron-lifetime data Coleman *et al.*¹³ estimated that the total excitation cross section at 24.6 eV is about $0.14\pi a_0^2$, substantially higher than the present result. Resolution of the discrepancy may be achieved in the future by a direct measurement of the positronium-formation cross section.

The cross section for 2^1S helium excitation by electrons below 30 eV is about $0.025\pi a_0^2$,¹⁴ but the total singlet excitation cross section is about $0.1\pi a_0^2$ and the total (singlet+triplet) cross section about $0.2\pi a_0^2$. It is probable that the smaller positron cross sections reflect the smaller number of available excitation channels open to the positron.

Although the incident beam is typically attenuated by 25%, double or multiple scattering leads to possible errors on Q_{ex} of only a few percent. For a positron to be timed within the limits of the secondary peak its first collision must have been atomic excitation; elastic scattering (predominantly at large angle), ionization, or positronium formation would either increase the positron's TOF to beyond the limit of the excitation peak or remove the particle from the beam entirely. Because the scattered positron is left with low kinetic energy (2.4 to 9 eV) following excitation, the only channel then open for a second interaction is elastic scattering, with a lower cross section. Corrections to the measured peak intensities to allow for losses due to elastic scattering amount to less than 8% but have been applied in the calculation of the cross sections shown in Fig. 4. In an experimental check on multiple-scattering effects, cross sections at 25 eV, deduced from experimental runs using helium pressures of 0.1, 0.2, and 0.3 Torr (attenuating the incident

beam by 20%, 40%, and 55%, respectively) were found to agree within statistical errors.

Contributions to the error bars on the cross sections of Fig. 4 arise as follows: 1% and 5% statistical uncertainties in I_i and I_{ex} , respectively; 5% assessed systematic uncertainties in the subtraction of background components from beneath the secondary peaks; 5% in the values used for Q_T ; and 5% in the adopted nl value. Adaptation of the system to enable the observation of backscattered positrons is currently being pursued.

The authors wish to thank Dr. L. M. Diana for useful discussions, and D. Cook for assistance with data analysis. This work was supported in part by the Robert A. Welch Foundation, Houston, Texas 77002, and by the National Science Foundation Grant No. SPI-79-26970.

¹R. W. Bussard, R. Ramaty, and R. J. Drachman, *Astrophys. J.* **228**, 928 (1979).

²T. C. Griffith, G. R. Heyland, K. S. Lines, and T. R. Twomey, *J. Phys. B* **12**, L747 (1979).

³P. G. Coleman, J. D. McNutt, J. T. Hutton, L. M. Diana, and J. L. Fry, *Rev. Sci. Instrum.* **51**, 935 (1980).

⁴P. G. Coleman, J. D. McNutt, L. M. Diana, and J. R. Burciaga, *Phys. Rev. A* **20**, 145 (1979).

⁵J. M. Dale, L. D. Hulett, and S. Pendyala, to be published; L. D. Hulett, private communication.

⁶P. G. Coleman, T. C. Griffith, and G. R. Heyland, *Appl. Phys.* **5**, 223 (1974).

⁷P. G. Coleman, *J. Phys. E* **12**, 590 (1979).

⁸K. F. Canter, P. G. Coleman, T. C. Griffith, and G. R. Heyland, *Appl. Phys.* **3**, 249 (1974).

⁹T. S. Stein, W. E. Kauppila, V. Pol, J. H. Smart, and G. Jesion, *Phys. Rev. A* **17**, 1600 (1978).

¹⁰J. W. Humberston, in *Advances in Atomic and Molecular Physics*, edited by D. R. Bates and B. Bederson (Academic, New York, 1979), Vol. 15, p. 116.

¹¹D. Andrick, H. Ehrhardt, and M. Eyb, *Z. Phys.* **214**, 388 (1968).

¹²S. Trajmar, *Phys. Rev. A* **8**, 191 (1973).

¹³P. G. Coleman, T. C. Griffith, G. R. Heyland, and T. L. Killeen, *J. Phys. B* **8**, L185 (1975).

¹⁴F. J. de Heer and R. H. J. Jansen, *J. Phys. B* **10**, 3741 (1977).